High-capacity dynamic indoor all-optical-wireless communication system backed-up with millimeter-wave radio techniques

High-Capacity Dynamic Indoor All-Optical-Wireless Communication System Backed-up with Millimeter-Wave Radio Techniques

K. A. Mekonnen, *Student member, IEEE,* E. Tangdiongga, *Member, IEEE*, and A. M. J. Koonen, *Fellow, IEEE, Fellow OSA*

***Abstract*— We propose a full-duplex dynamic indoor optical-wireless communication system using a crossed pair of diffraction gratings and photonic integrated circuits with multicasting capability of 10 Gb/s on-off-keying and >40 Gb/s discrete-multitone data per user, backed up by a 60-GHz radio fallback system, with shared capacity of ~40 Gb/s to realize reconfigurable and reliable high-capacity links to wireless users equipped with localization and tracking functionalities. The use of semiconductor optical amplifiers integrated with reflective electroabsorption modulators allows us to provide cost-efficient reflective transmitters at the user terminals in the upstream using centralized light sources and wavelength reuse technique. The 60-GHz radio fallback system allows us to cope with line-of-sight blocking in the optical-wireless links, thereby significantly enhancing the reliability of the wireless communication system.**

***Index Terms*—Indoor networks, free-space communication, beam steering, radio-over-fiber, reflective electroabsorption modulator, dynamic optical routing, optical carrier reuse.**

I. Introduction

Current indoor wireless networks are experiencing enormous pressure due to the exponentially rising number of mobile devices and the growing demand for high data rates per user [1]. 60-GHz and higher radio frequency (RF) bands have been investigated to tackle this. Using spatial multiplexing by means of radio beam-forming techniques high-speed wireless links can be provided to the individual users with reduced interference between them [2]. Dynamically routed radio-over-fiber (RoF) systems play an important role in transporting these broadband services to/from radio access points (RAPs) fixed in every room [3]. RoF techniques will enable low cost wireless links [4], but are limited by available bandwidth and regulation.

Wireless access to the fiber infrastructure using low complexity techniques is an active area of research. Recently, interest in optical-wireless communication (OWC) as a promising alternative to traditional radio frequency techniques is increasing significantly thanks to its unsurpassed high carrier frequencies that allow huge unlicensed bandwidths as well as immunity to electromagnetic interference. It can solve the looming RF spectrum crunch and interference problems in indoor environments. The visible and infrared regions are currently under investigation. Due to limited modulation bandwidth of light emitting diodes (LEDs), that are also used for widespread illumination, 10 Gb/s and higher transmission speeds are beyond the capability of visible light communication (VLC) [5,6]. Compared to VLC, infrared OWC (IOWC) systems can provide large capacities as well as the benefit of deploying the mature and widely available components in conventional optical fiber communication systems as well as a seamless integration into the future fiber-to-the-home (FTTH) infrastructure [7]. Using narrow infrared beams, ultrahigh unshared capacities can be provided to individual users. IOWC has attracted a significant research attention. To mention a few of the recent progresses: in [8], Wang et al demonstrated an IOWC system using diverging beams of footprint up to 1 m at 3 m free-space distance. 12.5 Gb/s transmission speed has been achieved using this system. By using collimated infrared pencil beams, Gomez et al showed a 100 Gb/s IOWC system over 3 m distance [9]. And more recently, we have demonstrated an IOWC system using arrayed waveguide gratings (AWGr) based beam steering, and optical beams of diameter 8 cm [10]. 112 Gb/s per user has been achieved using 4-level pulse-amplitude-modulation proving that a wireless system can have a comparable (or better) performance to a single-mode fiber transmission system.

A multibeam steering mechanism is needed at the RAPs to direct each optical pencil beam to the intended user. Several beam steering techniques have been proposed in the recent past for applications in indoor IOWC. In [8,11] micro-electromechanical mirrors, where each channel requires an individual mirror, are implemented to steer optical beams to indoor users. Liquid crystals as beam steering devices are also demonstrated in [12]. Another active 2D beam steering method was reported by Gomez et al by using spatial light modulators [9]. However, these devices have drawbacks such as the need for local powering, slow steering speed, and the need for separate control channels. Using remotely controlled passive dispersive components was proven to be beneficial since local powering is not needed and control complexity is reduced [13,14]. In this work we implement the 2D beam steering module (by cascading two diffraction gratings perpendicularly)

Manuscript received February 01, 2018; revised May 13, 2018; accepted June 12, 2018. This work was supported by the European Research Council under the Advanced Grant project BROWSE – Beam-steered Reconfigurable Optical-Wireless System for Energy-efficient communication.

K. A. Mekonnen, E. Tangdiongga and A. M. J. Koonen are with the Institute for Photonic Integration, Eindhoven University of Technology, Eindhoven, The Netherlands (e-mail: k.a.mekonnen@tue.nl, e.tangdiongga@tue.nl, a.m.j.koonen@tue.nl).

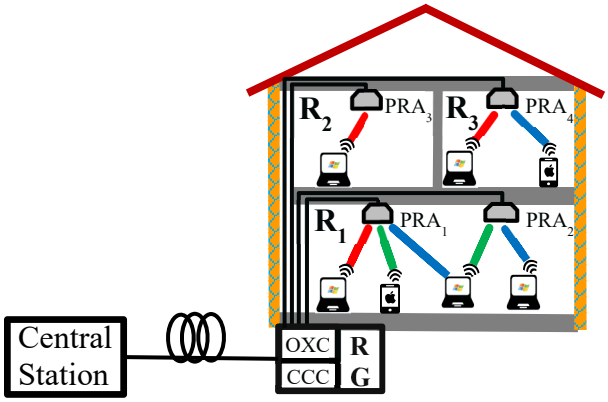

Fig. 1 Proposed in-building network architecture.

that we studied previously [14,15] to achieve all-optical-wireless bidirectional communication using different modulation formats, and all-optical multicasting of signals sent from a central site. In addition, a radio back up system that doesn't need beam steering is also demonstrated. Since the backup link is intended as a fallback, a lower communication speed is acceptable for the users. Moreover, dynamic routing is key for ensuring capacity-on-demand, to minimize power consumption, and handle link failures.

In our previous work, we proposed a dynamic routing mechanism using a semiconductor optical amplifier (SOA) based all-optical wavelength conversion followed by wavelength based 2-dimentional beam steering using a crossed pair of diffraction gratings [16]. However, since a fixed waveband, determined by the AWGr, is allocated per RAP, it was not possible to provide dynamicity in the network for capacity on demand. In addition, the network only demonstrated the routing of signals sent from a central site. In [17,18], we implemented a multicast capable 4×4 SOA-based optical-cross-connect (OXC) chip to route optical-wireless and 60-GHz radio signals to the access points. Deploying photonic-integrated-chips (PICs) for indoor communications is highly beneficial due to their compactness and low power consumption. Moreover, multicasting capabilities of bandwidth-hungry services such as 4K/8K ultrahigh-definition television (UHD-TV) is a potentially essential function in indoor networks. All-optical multicasting in intelligently routed wireless network provides reconfigurable network connectivity and reduction of cost and power consumption.

In this paper, we demonstrate a novel dynamic full-duplex indoor all-optical-wireless communication system with multicasting capability backed up by a millimeter-wave (MMW) RoF system to realize highly reconfigurable and reliable wireless links which provide ultimate capacities per user. The paper builds on the system we presented in [18]. All-optical multicasting of up to 40 Gb/s wireless data per user is demonstrated employing a wavelength selective OXC chip and cross-gain-modulation (XGM) using an SOA. By using rate-adaptive discrete-multitone (DMT) modulation, full-duplex optical-wireless transmission rates ~40 Gb/s per user are demonstrated. Additionally, a shared capacity of >35 Gb/s was achieved in the 60-GHz radio fallback system.

In comparison to 60-GHz radio communication system, which has been a hot research topic in the radio domain, we believe that, in addition to the significantly higher unlicensed bandwidth (10 – 100 GHz) that it provides, our OWC system is more cost efficient and scalable, especially when there are a high number of RAPs in the system. The radio beam-steering necessary to provide the available capacity in the 60-GHz region to individual users increases power consumption and complicates the RAPs and user terminals. Our optical beam steering module does not need local powering and allows us to control the steering remotely by changing the wavelength.

II. Indoor Network Architecture

The proposed in-building network architecture is depicted in Fig. 1. The residential gateway (RG) acts as the interface between the access network and the indoor network. Each room is equipped with one or more access points, called pencil radiating antennas (PRAs), to direct wireless signals to/from the individual users. As shown in Fig. 2 dynamic routing of downstream optical pencil-beams to the individual rooms via an optical fiber backbone network is performed using an OXC in the RG. Network control and management (C&M) functions such as communication protocols, routing logics, autonomous resource management, and user localization and tracking are carried out by the central communication controller (CCC) at the RG. The wireless channel is realized by implementing line-of-sight (LOS) infrared pencil beams with wavelengths beyond 1.4 μm, where eye safety regulations allow higher beam powers than in the visible range (up to 10 mW is allowed according to ANZI Z-136 and IEC 60825 standards).

The PRAs consist of 2D beam steering devices in order to direct the LOS beams from/to the RG to/from the users (see Fig. 2). Desirable characteristics for selecting a steering method

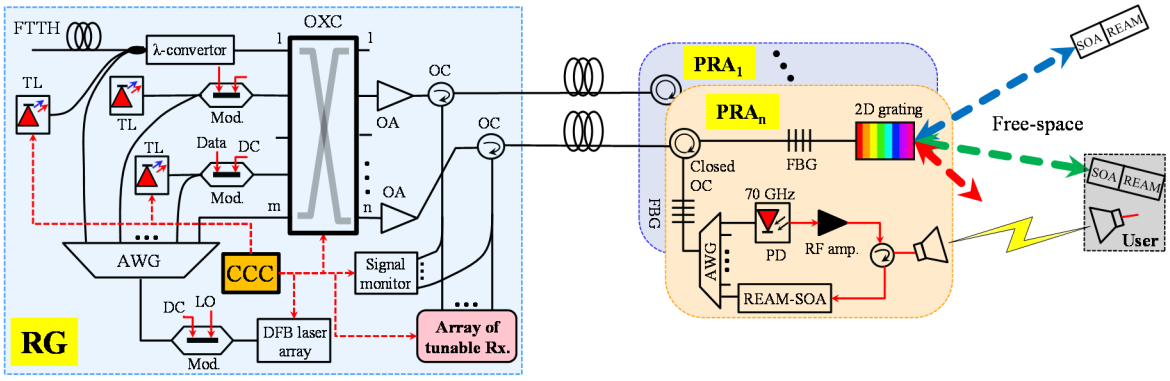

Fig. 2 OXC based dynamic and reliable bidirectional optical/radio wireless network employing optical wireless and 60-GHz RoF techniques.

include the ease of installation, enabling plug-and-play (without any local processing and local powering), fast steering speed, low power consumption, ability for simultaneous steering, low loss in the wavelength range of operation, accuracy and reliability, and good coverage area. Considering these key characteristics, we have proposed the use of passive diffraction gratings for beam steering, in cooperation with remote wavelength-tuned source at the RG [14]. Array of tunable laser (TL) or distributed feedback laser (DFB) diodes can be implemented as optical sources to serve the users with appropriate wavelengths for the beam steering. The 2D beam steerers are realized by cascading two diffraction gratings perpendicularly [7]. As the gratings diffract different wavelengths to different directions, the steering can be controlled remotely by tuning the wavelengths. The downstream optical carriers are reused for upstream communication at the user device after data erasure using a reflective electroabsorption modulator monolithically integrated with an SOA (REAM-SOA).

To tackle outages in the optical-wireless links, due to LOS blocking, a MMW radio protection scheme is implemented. This allows us to support communication at lower speeds until the optical-wireless link is reestablished and normal operation resumes. An optical up-conversion technique using a Mach-Zehnder modulator (MZM) is implemented to generate the MMW radio signals from the baseband signals [19]. A single MZM can be used to generate multiple downstream MMW wireless channels at the same time as shown in Fig. 2.

The proposed system allows us to realize simple PRAs for high-capacity IOWC system by moving all the complexities from the PRAs to the RG, where costs are shared. The OXC enables us to support capacity-on-demand, and share the tunable transceivers between the users. The main complexity in the PRAs come from the MMW components such as high-speed photodiodes, power amplifiers and low-noise-amplifiers (LNAs) for the MMW backup system. However, these components are intended for only backup purposes. A key drawback of IOWC using narrow beams is its susceptibility to LOS blocking, which necessitates alternative means to cope with connection interruptions. Currently, we are working on integrated 60-GHz phased array antenna (PAA) system where the discrete 60 GHz components are integrated together to realize a compact and simplified PRA [20].

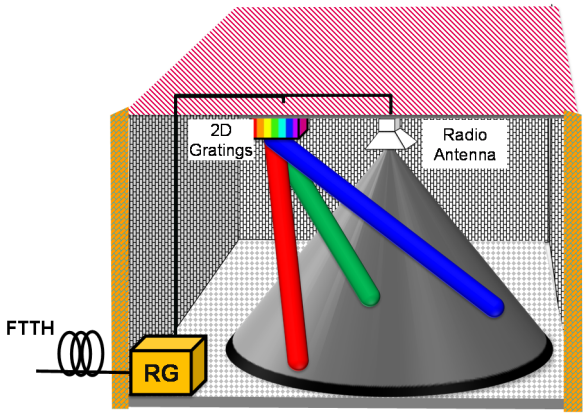

Fig. 3 Shared radio wireless communication with large beam footprint to tackle LOS blocking in the optical-wireless links.

III. MMW Radio Fallback System

The optical-wireless communication link is established by first obtaining the location of the users. This can be done by implementing radio/optical based localization techniques [21,22]. The position of the user determines the wavelength needed for the optical-wireless communication. By means of radio based localization techniques, the CCC can store a lookup table of location-wavelength mapping, for example, that can be populated by means of fingerprinting, and can be accessed to estimate the wavelength associated to a particular location within the coverage area. Optical techniques can then be implemented to fine tune the wavelength. The localization system in the BROWSE project, which is an ongoing work in another part of the project, is based on this principle.

Optical-wireless links are prone to link outages due to LOS blocking. To tackle this, we have implemented a MMW radio system to provide the user a lower speed alternative. When the CCC/user detects a link-failure to any user served by any PRA, it activates the MMW radio fallback channel to that PRA. MMW radio signals are less susceptible to LOS issues compared to optical-wireless signals, because of their large footprint (see Fig. 3). In [23] we demonstrated a 60-GHz radio system as a backup to the optical-wireless links. However, it was not possible to provide protection to more than one optical-wireless link at a time, and the radio beam steering led to a more complicated transceiver hardware at the RAPs and user terminals, where simplicity is a critical requirement.

In this work, we demonstrate a simple 60-GHz protection system which is only operational when there are failures in the optical wireless links. Though any RF band, such as 5-GHz, 10-GHz or above, could be considered for the radio backup link, the 60-GHz region was chosen as this region provides 7-GHz unlicensed bandwidth. To completely remove the impact of the LOS blocking (also for the 60-GHz signal), the radio antenna and 2D gratings at the PRA can be kept at different locations. The radio footprint is designed to cover the entire optical-wireless coverage area in the room (see Fig. 3). Hence, no beam steering is required for the radio fallback system which simplifies the access point and user terminals. This can be achieved by using broadcast antennas (hence, with lower directivity or gain). The directivity, D of an antenna is given by:

$$D = \frac{4\pi A}{\lambda^2} \tag{1}$$

where A is the effective antenna aperture, and λ is the operating wavelength. The antenna gain is defined as its directivity taking into account its efficiency, η.

$$G = \eta \mathrm{D} = \eta \frac{4\pi A}{\lambda^2} \tag{2}$$

On the other hand, lower antenna gains results in lower received signal power, which in turn results in reduced data transmission speeds. The received signal power decreases

quadratically with increase in signal frequency and distance between the transceivers. From Friis transmission equation:

$$P_{rx} = P_{tx} G_{tx} G_{rx} \left(\frac{\lambda}{4\pi d}\right)^2 \quad (3)$$

where P_{tx} and P_{rx} are the transmitted and receive signal powers, respectively, G_{tx} and G_{rx} are the transmitter and receiver antenna gains, and d is the free-space distance between the transmitter and receiver antennas.

Hence, using broadcast 60-GHz antennas (with less gain) means reduced reach/capacity. Moreover, the total capacity will be shared among the users in the room using a suitable medium-access control protocol. However, since the radio system is intended for only backup purposes and LOS blocking doesn't happen frequently, communication at a lower speed is acceptable until the optical-wireless link is operational again.

For a certain frequency range, the gain of an antenna is directly proportional to its aperture. The beamwidth of the radiation, which is inversely proportional to its directivity (or aperture) can be calculated from:

$$BW_\theta \, BW_\phi = \frac{52525}{\mathrm{D}} \quad (4)$$

where BW_θ and BW_ϕ are the elevation and azimuth 3-dB beamwidths (in degrees). Here we approximated the radiation pattern with an ellipse. The number 52525 in (4) comes from the conversion from radians to degrees in the beamwidth calculation for elliptic antenna patterns. Hence, to cover a wider area, the antenna aperture should be smaller.

In practical deployments of such a system, the aperture of the antennas used should be designed taking into consideration the operating frequency, the received power (which is related to the data transmission speed) and the room size. In our system we implemented a simple 60-GHz pyramidal horn antenna of aperture (~2 cm ×2.5 cm), which results in approximately 20 dBi gain, at both the PRA and user terminal. Using (3) and (4), the resulting free-space path loss (at 2.5 m distance) and 3-dB beamwidth are approximately 35 dB and 15° ×15°, respectively. LNAs are implemented to cope with the free-space losses. In comparison, our 2D beam steered OWC system has a coverage angle of 5.6° ×12.2° without angular magnification [7]. This means that a single antenna radiation pattern can act as a protection link to multiple optical-wireless links, albeit at lower communication speeds. A dipole antenna (or an antenna with a smaller aperture) would give a lower gain or larger beam width but at the expense of reduced received signal power.

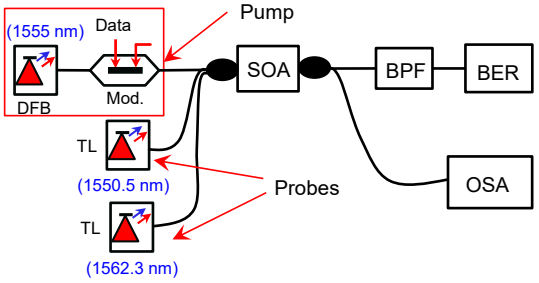

Fig. 4 XGM based wavelength conversion using an SOA.

The 60-GHz radio signals are generated by up-converting the baseband data optically at the RG using DFB lasers and a single MZM implementing optical carrier suppression technique. Compared to other modulation schemes to generate MMW radio signals, this scheme has a simple configuration and relaxed-frequency bandwidth requirements for electrical and optical components, and results in better receiver sensitivity [19]. Since the MZM can up-convert multiple signals to MMW frequency by using different wavelengths, it allows us to provide multiple protection channels to multiple rooms at a time. An AWG in combination with the OXC then routes the generated radio signals to the PRAs as shown in Fig. 2. Suitable fiber Bragg gratings (FBGs) at the PRAs separate the optical-wireless links from the 60-GHz signals which are received by a high-speed photodetector through another AWG. To avoid any tunable component at the PRAs, a fixed range of wavelengths, determined by the bandwidth of the FBG, is implemented for the RoF system. One DFB laser at the RG, multicasting its output to the PRAs, can be shared among the PRAs to transport upstream radio signals using a REAM-SOA [24].

The switching between the optical-wireless and MMW channels is governed by the control plane. Control messages are exchanged periodically between the user and the CCC. If the CCC does not receive an acknowledgement from the user, it considers the IOWC link to be blocked. The user, which monitors the received optical power, also considers the link to be broken when it does not detect the optical signal. The CCC periodically checks if the IOWC link is operational again by activating the TL that was serving the user before the LOS blocking. When the user detects an optical signal, it can inform the CCC about it in the acknowledgment message via the radio link, and then the IOWC link can be re-established. If the user changes its location while it is under LOS blocking, then the localization should be performed again in order to re-establish the higher capacity IOWC link. Once the new location of the user (hence the new wavelength) is known, the RG checks if the IOWC link can be established using the new wavelength. If it is not possible, then the user is assumed to still be under LOS blocking, and the radio communication will be retained.

IV. Indoor All-Optical-Wireless Multicasting

Point-to-multipoint communication of bandwidth intensive services such as video conferencing, video-on-demand, and UHD-TV is a potentially essential function in indoor networks. Recently, a point-to-multipoint IOWC system that allows multicasting functionality has been demonstrated by means of an SLM in a spatial division mode [25]. All-optical multicasting, where the data on a signal at a given wavelength

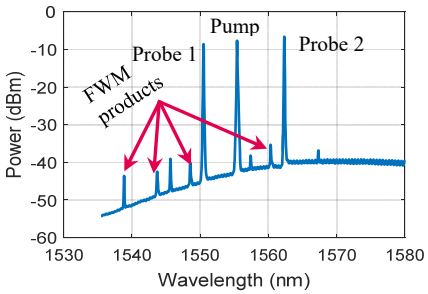

Fig. 5 XGM output optical spectrum.

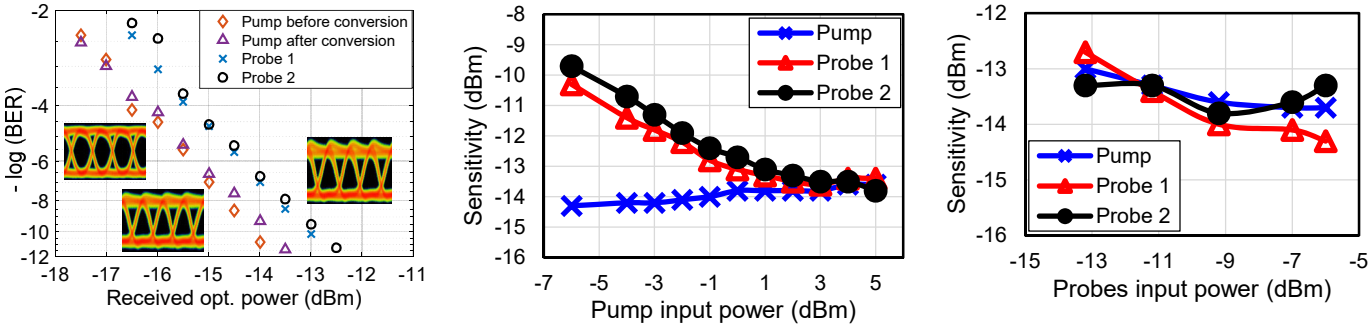

(a) (b) (c)

Fig. 6 XGM based wavelength conversion results: (a) BER curves for the pump and probe signals (inset: eye diagrams); (b), (c) receiver sensitivity measurements (at BER of 1×10^{-9}) when the input optical powers for the pump and probes are varied, respectively.

is simultaneously replicated onto multiple predetermined wavelengths, in intelligently-routed indoor wireless network provides reconfigurable network connectivity and capacity, reduction of power consumption and flexibility in operation.

In our 2D gratings based beam steered system, any indoor location corresponds to a specific wavelength. Hence, to route a signal sent from a central site (such as a UHD video signal) to the appropriate user (or multiple users), wavelength conversion will be necessary. Access networks and indoor environments typically require simple, low cost, yet high performance and reliable systems. Oftentimes, on-off-keying (OOK) modulation-direct detection (DD) transceiver designs are preferred. Of all the techniques of wavelength conversion for intensity modulated signals, the XGM mechanism in SOAs has shown very robust operation over a wide spectral range with high speed [26]. Moreover, its simplicity and ability to convert to multiple wavelengths at the same time make it an attractive solution for all-optical routing and multicasting in indoor networks. By optimizing the input optical powers of the pump and probe signals, multicasting to multiple probe sources within the gain bandwidth of the SOA is possible as demonstrated in [27]. The number of users that can be supported is practically limited by the low output optical power levels for the individual signals from the SOA, which can be overcome by including an additional optical amplifier after the wavelength conversion. Additionally, nonlinearities that arise from the interaction of the (many) probe signals may also limit the number of users. To tackle this, an additional SOA can be implemented. As shown in the experimental setup in Fig. 7, the SOA can be shared dynamically by connecting it between one output and input ports of the OXC, where the input port to which it is connected is capable of wavelength selective routing. Note that multicasting over the MMW fallback channel is also possible with the proposed system (see Fig. 2 and Fig. 7). Theoretical background work in XGM based wavelength conversion has been carried out in previous publications [28]. Here, we carried out experiments to validate the XGM based wavelength conversion for indoor service multicasting in our 2D beam-steered OWC system.

Fig. 6a shows the bit-error-rate (BER) curves measured using the pump (signal)-probe experimental setup depicted in Fig. 4 when the XGM operation was optimized for the least crosstalk from FWM products generated by the XGM process, and the best efficiency. The FWM products that might interfere with other optical-wireless signals (at the same wavelengths) were at least 30 dB weaker than the desired signals (see Fig. 5). The SOA was biased at 350 mA, and the input optical power was -+1 dBm for the pump of wavelength 1555 nm and -7 dBm for each of the two probe wavelengths (at 1550.5 nm and 1562.3 nm). Conversion penalty of ~1 dB was measured at BER of 1×10^{-9} in this operation condition, while the pump remained virtually unaffected. The influence of the input optical power of the pump and probe sources can be seen in Fig. 6b and c. As illustrated in Fig. 6b, for fixed input optical power of -7 dBm for each of the probe sources, the receiver sensitivity (at BER of 1×10^{-9}) of the converted wavelengths improved by ~5 dB when the input optical pump power was increased from -6 dBm to 5 dBm. On the contrary, for a fixed input optical power of -1 dBm for the pump signal, the sensitivity of the converted signals only improved by ~1.5 dB when the input optical power for each of the probe sources was increased from -13 dBm to -6 dBm. It should be noted that increasing the input optical signal power (i.e., the pump power) also results in enhancement of FWM products. Hence, system implementation requires that the input optical power levels for the pump and probe sources be optimized for least FWM products and better conversion efficiency. The SOA bias current of 350 mA was chosen because the high bias current, accompanied by injection of a high power optical beam, can result in conversion speeds significantly greater than the carrier recovery rates [28]. An increase in SOA bias current and the input optical power results in a reduction in the effective response time of the carriers and consequently a larger modulation bandwidth.

V. Experimental Demonstration

Figure 7 illustrates the proof-of-concept experimental setup. A 4×4 OXC chip was used at the RG to route signals to the intended PRAs. The OXC chip was a broadcast and select switch consisting of a 1:4 splitter, a wavelength selective switch (WSS) and an 4:1 combiner on each path. Each WSS comprises SOA-gate switches and AWGrs to select one or more wavelength channels and forward them to the output ports according to the control signals. The OXC chip was designed by Calabretta et al and has dimensions of 6 mm × 4 mm [29]. Fabrication of the chip was realized employing the multi-project wafer run in the JEPPIX platform. Booster SOAs are included at the input ports to minimize the insertion losses, mainly from the AWGrs. Each AWGr has an FSR of 15 nm and are designed with channel bandwidth of 1.4 nm and channel

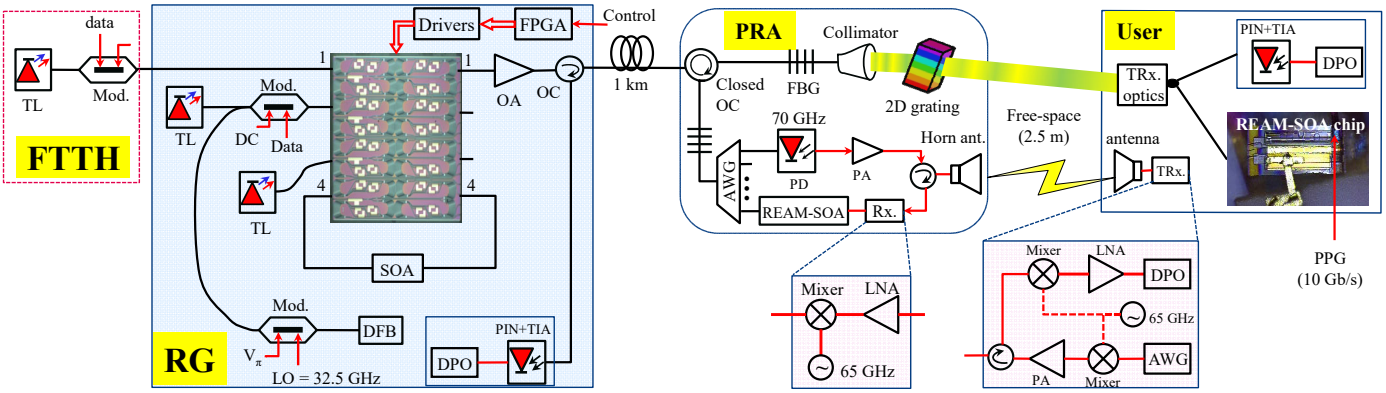

Fig. 7 Experimental setup using a 4×4 OXC chip for dynamic routing and an SOA for wavelength conversion at the RG, a 2D gratings module at the PRA for optical pencil-beam steering to users, and a REAM-SOA and 60-GHz components for upstream SCM-RoF transmission at the PRA and user terminal.

spacing of 4 nm, taking into consideration the limited cell size (6 mm × 4 mm) offered in the multi-project wafer run. The details about the design, fabrication process and characterization of the OXC chip can be found in [29,30].

An FPGA was used to control the OXC chip to achieve the desired switching functionalities by activating the appropriate gating SOAs in the OXC chip. After amplification by an erbium-doped fiber amplifier (EDFA) to compensate the 16 dB loss introduced by the OXC chip, the 2D gratings, and coupling optics, the signal was launched into a 1km fiber, and then steered by the 2D gratings to the PIN+TIA receiver located at a free-space distance of 2.5m.

A. Indoor optical-wireless multicasting

The 2D beam steering module was constructed by cascading a reflective blazed grating of FSR ~16 nm with a fused silica transmission grating of FSR ~125 nm perpendicularly [7]. With this arrangement we have achieved a coverage angle of 5.6° × 12.2° corresponding to a 24.5 cm × 54 cm area at a free-space distance of 2.5 m without angular magnification. The steering module has a 3-dB pass bandwidth of approximately 10 GHz [7]. The spectral width is limited by the dispersion of the two gratings and the small aperture of the receiver collimator implemented to focus the narrow optical beam onto the fiber-pigtailed photoreceiver. The collimator's reception angle is very limited (field-of-view < 0.034°).

In order to stay within the eye safe limit, in all of our experiments, the transmitted optical power in the OWC link was not more than 8 dBm, resulting in a maximum received optical power of +2 dBm at the user terminal. The total end-to-end free-space loss of the OWC channel was approximately 6 dB, including alignment and reflection losses. Although we performed the experiment for a free-space distance of 2.5 m, the performance variation is negligible within a typical indoor scenario (room size <10 m) since collimated narrow beams (beamwaist ~3.3 mm) were deployed for the communication.

When a signal sent from the central site needs to be multicasted to multiple users, it will be switched to the last port of the OXC chip. The signal then mixes with continuous wave (CW) probe signals that are also switched to this last port so that the data will be copied to the probe signals using XGM via an SOA. The multicast data were then routed again by the OXC chip to the intended PRAs/users. The OXC chip allows us to share the SOA and tunable laser sources among multiple users in the system, and to route the individual signals to the appropriate PRAs (see Fig. 7) in a dynamic, and energy and cost efficient manner. Here, an optical signal at 1555.5 nm wavelength, bearing a 10 Gb/s OOK or 10 GHz wide DMT data, emulates the data to be multicast. Two CW TLs (tuned at 1550.5 nm and 1562.3 nm) were used as probe signals. Note that the wavelengths of the CW light sources are determined by the CCC after user localization. The SOA was biased at 350 mA and, for the best results, the input pump and probe signal powers were fixed at -1 dBm and -6 dBm, respectively.

In the upstream, the downstream optical carrier was reused after the data on it was erased by an SOA working in its saturation region [31], with the input optical power fixed at -5 dBm. The REAM-SOA at the user terminal was then used to modulate the upstream data on the recovered optical carrier. The modulation format used was 10 Gb/s OOK when OOK was used for the downstream and 10 GHz wide DMT when DMT was used for the downstream. A PIN+TIA photo-receiver was used for both downstream and upstream communications.

As shown in Fig. 5 FWM products generated by the XGM process, that might interfere with other signals, were >30dB weaker than the desired signals since the XGM operation was optimized for the least cross-talk and the best efficiency. Fig. 8 shows the BER curves of the multicast operation when 10 Gb/s OOK was implemented. The XGM operation introduced a 1 dB penalty at BER of 1×10^{-9} for the original signal as depicted in Fig. 8a. The penalty introduced by the optical fiber cable to the RG was less than 0.5 dB. Compared to the original, penalties of 0.5 dB and 1 dB were observed for the two probe signals (see Fig. 8b). The transmission link to the wireless users through the OXC chip introduced an additional 1.5 dB penalty for all the channels due to ASE noise from the gate SOAs used in the OXC chip and the XGM process, and the noise added by other components in the optical path. Nevertheless, the total penalty introduced was below 2.5 dB for all channels. When 10 GHz wide DMT signal was implemented, the wavelength conversion process resulted in a reduction of 7 Gb/s in the achievable data rate. 36 Gb/s transmission rate was measured using the XGM based wavelength conversion. Fig. 9c shows the achievable data rate curves for the downstream and upstream without

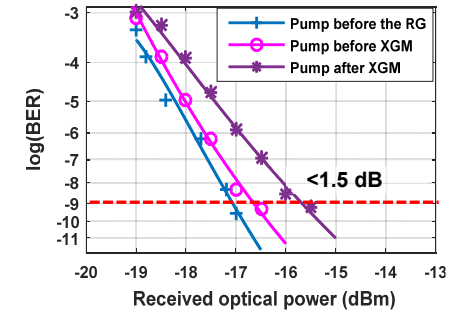

(a)

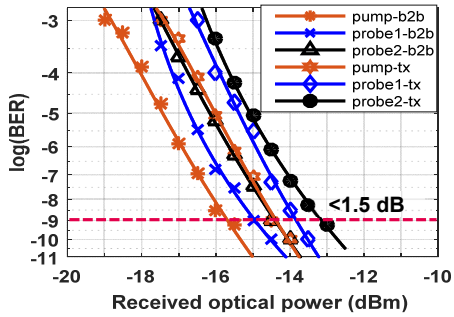

(b)

Fig. 8 BER curves: (a) of the pump signal before and after XGM, and after the OXC-chip; (b) of the pump and probe signal before and after transmission.

wavelength conversion.

The BER curves in Fig. 9b illustrate the integrity of the 10 Gb/s upstream OOK data. The sensitivity of the PIN+TIA at BER of 1×10^{-9} was measured to be -16.5 dBm when a clean optical carrier was used. A 3 dB penalty was measured when the optical carrier recovered from the downstream transmission using an SOA biased at 450 mA and input optical power of -5 dBm was used. The extinction ratio of the downstream signal was kept at 8 dB for best results. Under this operation condition, the SOA erased the modulation from 300 mV (peak-to-peak) to <20 mV as demonstrated in Fig. 9a. The SOA was able to suppress the downstream modulation by 10 dB. Increasing the input optical power to the SOA and/or its bias current improves its ability to erase the modulation on the optical carrier since this puts the SOA in deep saturation (see Fig. 9a).

B. 60-GHz radio fallback system

The 60-GHz radio protection system was also evaluated using the setup in Fig. 7. A DFB laser at 1529 nm was modulated by a 32.5 GHz radio tone using a MZM biased at its null-point to generate 65 GHz spaced tones which were then modulated by the wireless data and routed to the PRA via the OXC chip. This signal was then received by a 70 GHz photo-diode and radiated to the user using a horn antenna. The output of another DFB laser at 1530 nm was sent to the PRA via the AWG and OXC chip, reflected by an FBG at the PRA, and subsequently modulated by the down-converted upstream radio data using the REAM-SOA [24]. The bandwidth of the FBG used in the experiment was 3 nm at 1530 nm central wavelength. Discrete 60 GHz components were used in the experiment as shown in the inset of Fig. 7.

Because of unavailability of smaller antennas at the time of the experiment, we used fairly directive horn antennas with apertures of 4 cm × 6 cm resulting in a gain of ~ 25 dBi at the transmitting and receiving ends. The transmitted power was +5 dBm. The received power can be calculated using (3) to be approximately -18 dBm at a free-space distance of 2.5 m. The 3-dB beamwidth is ~ 10° ×10°, corresponding to a footprint of 44 cm × 44 cm at 2.5 m distance between the transceivers (the optical-wireless coverage area is 24.5 cm × 54 cm). The gain of the LNAs used was 20 dB. In practical deployments antennas with lower gains can be employed to increase the coverage area. This, however also decreases the available data rate for individual users as the whole capacity will be shared between all the users in the coverage area, and the received signal power will be significantly lower. Transmission at lower speeds is acceptable until the optical-wireless channel is re-established.

The capacity of the MMW radio backup system, measured for the best placed user, was measured to be 34 Gb/s for the downstream and >45 Gb/s for the upstream at an average BER $<4.1\times10^{-3}$. The downstream showed worse performance than the upstream because of the ASE noise of the SOAs in the OXC chip and penalties due to the MMW conversion process, which is also visible in the signal-to-noise ratio (SNR), and bit-loading profile plots shown in Fig. 10b. As shown in Fig. 10a, an optical carrier suppression ratio of 18 dB was achieved for the downstream using a single-drive MZM. The transmission capacity will change if the user is at a different location within the 3-dB coverage area because the received power will change by up to 3 dB. Thus, we expect lower transmission rates at locations far from the center of the beam. The measured transmission capacity here can act as the maximum transmission capacity that can be provided to individual users using the MMW fallback system. Currently, we are developing

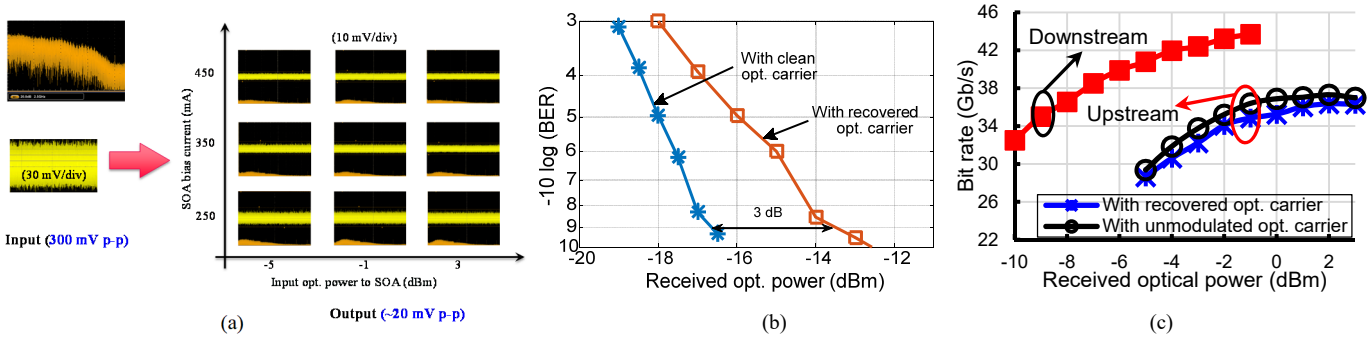

(a) (b) (c)

Fig. 9 (a) Saturated SOA based optical intensity modulation erasure: waveforms at the input and output of the saturated SOA at different bias currents and input optical powers; (b) BER curves for the upstream optical wireless 10 Gb/s OOK data; (c) Downstream and upstream achievable data rates as a function of received optical power with optical carrier reuse when the saturated SOA was biased at 450 mA and the input optical power was 0 dBm.

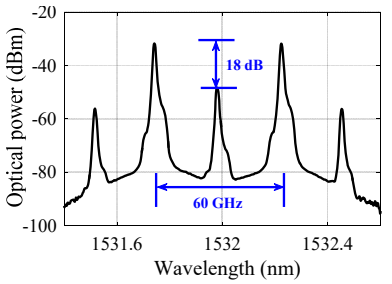

(a)

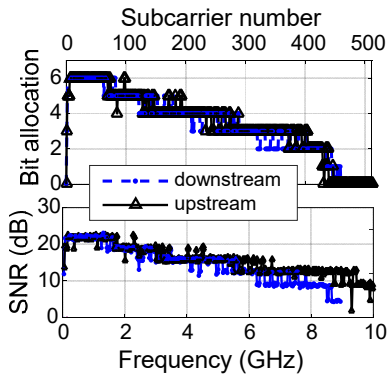

(b)

Fig. 10 (a) Optical spectrum of the downstream 60-GHz radio signal; (b) SNR, and bit-loading profile of the downstream and upstream 60 GHz radio signals.

an integrated PAA system to realize a compact and cost/energy-efficient 60-GHz system [20]. The PAA system can be tuned to provide wider or narrower beams according to our need by turning on/off PAA elements. It also allows us to perform user localization. This work is still on going.

VI. Conclusion

We presented a highly dynamic full-duplex indoor optical-wireless network with multicasting capability of 10 Gb/s OOK and ~40 Gb/s DMT data employing PICs to provide low cost/power consumption. A 60-GHz radio backup system with single beamwidth of 10° ×10° (corresponding to a footprint of 1 m × 1 m) and data capacity of >40 Gb/s at 2.5 m distance was also demonstrated to tackle optical-wireless link outages. Using REAM-SOAs at the PRAs and user terminals allows us to provide cost-efficient reflective transmitters using centralized light sources and wavelength reuse technique.

Acknowledgment

We would like to thank the III–V Lab, Alcatel-Thales, France for providing the REAM-SOA chips, and Dr. Nicola Calabretta for providing the OXC chip.

References

[1] M. Paolini, "Beyond data caps," Senza Filli Consulting, 2011.
[2] T. Nitsche *et al*, "IEEE 802.11ad: directional 60 GHz communication for multi-Gigabit-per-second Wi-Fi," *IEEE Commun. Mag.*, vol. 52, no. 12, pp. 132–141, Dec. 2014.
[3] A. M. J. Koonen and E. Tangdiongga, "Photonic home area networks," *J. Light. Technol.*, vol. 32, no. 4, pp. 591–604, Feb. 2014.
[4] N. Ghazisaidi and M. Maier, "Fiber-wireless (FiWi) access networks: challenges and opportunities," *IEEE Netw.*, vol. 25, no. 1, p. 36–42, 2011.
[5] D. O'Brien et al., "High-speed optical wireless demonstrators: Conclusions and future directions," *J. Lightw. Technol.*, vol. 30, no. 13, pp. 2181–2187, Jul. 2012.
[6] H. Haas, "Visible light communication," in *OFC*, Los Angeles, CA, 2015, Paper Tu2G.5.
[7] A. M. J. Koonen *et al*, "Ultra-high capacity indoor optical wireless communication using 2D-steered pencil beams," *J. Light. Technol.*, vol. 34, no. 20, pp. 4802–4809, Jun. 2016.
[8] K. Wang *et al*, "High-speed optical wireless communication system for indoor applications," *IEEE Photonics Technol. Lett.*, vol. 23, no. 8, pp. 519-521, Apr. 2011.
[9] A. Gomez *et al.*, "Beyond 100-Gb/s indoor wide Field-of-View optical wireless communications," *IEEE Photonics Technol. Lett.*, vol. 27, no. 4, pp. 367–370, Feb. 2015.
[10] F. Gomez Agis *et al*, "112 Gbit/s transmission in a 2D beam steering AWG- based optical wireless communication system," in *ECOC*, Gothenburg, Sweden, 2017, paper Th.2.B.1.
[11] P. Brandl *et al*, "Optical wireless communication with adaptive focus and MEMS-based beam steering," *IEEE Photonics Technol. Lett.*, vol. 25, no. 15, pp. 1428-1431, Aug. 2013.
[12] P. F. McManamon *et al*, "Optical phased array technology," *Proc. of the IEEE*, vol. 84, no. 2, pp. 268-298, Feb. 1996.
[13] T. Chan, E. Myslivets, and J. E. Ford, "2-Dimensional beamsteering using dispersive deflectors and wavelength tuning," *Opt. Express*, vol. 16, no. 19, pp. 14617, Sep. 2008.
[14] A. M. J. Koonen *et al*, "Reconfigurable free-space optical indoor network using multiple pencil beam steering," in Proc. *OECC*, 2014, pp. 204–206.
[15] A. M. J. Koonen, *et al* "Ultra-high capacity indoor optical wireless communication using 2D-steered pencil beams," in *MWP*, Paphos, 2015, WeC-5.
[16] K. A. Mekonnen *et al*, "Reconfigurable optical backbone network for ultra-high capacity indoor wireless communication," in *MWP*, Long Beach, CA, 2016, pp. 35–38.
[17] K. A. Mekonnen *et al*, "PIC-enabled dynamic bidirectional indoor network employing optical wireless and millimeter-wave radio techniques," in *ECOC*, Dusseldorf, 2016, pp. 500–502.
[18] K. A. Mekonnen *et al*, "High-capacity dynamic indoor network utilizing optical wireless and 60-GHz radio techniques," in *MWP*, Beijing, China, 2017, paper We2.3.
[19] Z. Jia *et al*, "Key enabling technologies for optical wireless networks: Optical millimeter-wave generation, wavelength reuse, and architecture," *J. Light. Technol.*, vol. 25, no. 11, pp. 3452–3471, Nov. 2007.
[20] B. Wang et al., "A 60 GHz phased array system evaluation based on a 5-bit phase shifter in CMOS technology," in Symp. Commun. Veh. Technol., Mons, Belgium, 2016, pp. 1–4.
[21] F. Winkler *et al*, "An indoor localization system based on DTDOA for different wireless LAN systems," in *WPNC*, Hannover, 2006, pp. 117.
[22] K. Wang *et al*, "Optical wireless-based indoor localization system employing a single-channel imaging receiver," *J. Light. Technol.*, vol. 34, no. 4, pp. 1141–1149, Feb. 2016.
[23] K. A. Mekonnen *et al*, "High-capacity dynamic indoor network employing optical-wireless and 60-GHz radio techniques," *J. Light. Technol.*, vol. 36, no. 10, pp. 1851–1861, May 2018.
[24] K. A. Mekonnen *et al*, "Integrated optical reflective amplified modulator for indoor millimetre wave radio-over-fibre applications," *Electron. Lett.*, vol. 53, no. 4, pp. 285–287, Feb. 2017.
[25] A. Gomez *et al*, "Point-to-multipoint holographic beamsteering techniques for indoor optical wireless communications," *Proc. of SPIE*, vol. 9772, pp. 97720Q, 2016.
[26] S. L. Danielsen, *et al*, "Bit error rate assessment of a 40 Gbit/s all-optical polarization independent wavelength converter," in *OFC*, San Jose, CA, 1996, paper PD12.
[27] K. Lee *et al*, "Multicasting in WDM-PON using cross-gain modulation in semiconductor optical amplifier," in *ECOC*, Turin, Italy, 2010, Mo.1.B.6.
[28] M. Asghari *et al*, "Wavelength conversion using semiconductor optical amplifiers," *J. Light. Technol.*, vol. 15, no. 7, pp. 1181-1190, Jul. 1997.
[29] N. Calabretta *et al*, "Monolithically integrated WDM cross-connect switch for nanoseconds wavelength, space, and time switching", in *ECOC*, Valencia, Spain, 2015, paper Mo.3.2.2.
[30] N. Calabretta *et al*, "Monolithically integrated WDM cross-connect switch for high-performance optical data center networks," in *OFC*, Los Angeles, CA, 2017, Tu3F.1.
[31] H. Takesue and T. Sugie, "Wavelength channel data rewrite using saturated SOA modulator for WDM networks with centralized light sources," *J. Light. Technol.*, vol. 21, no. 11, pp. 2546–2556, 2003.